Leaching of Sulfadiazine and Florfenicol in an Entisol of Chicken-raising Orchard: Impact of Manure-derived Dissolved Organic Matter

Lanre Anthony Gbadegesin
Institute of Mountain Hazards and Environment Chinese Academy of Sciences
Xinyu Liu
Southwest Jiaotong University
Chen Liu (chen1017@imde.ac.cn)
Institute of Mountain Hazards and Environment Chinese Academy of Sciences
Xiangyu Tang
Institute of Mountain Hazards and Environment Chinese Academy of Sciences

Research Article

Keywords: Antibiotics, leaching, mass flux, manure, dissolved organic matter (DOM), natural rainfall

Posted Date: March 11th, 2022

DOI: https://doi.org/10.21203/rs.3.rs-1337929/v1

Abstract

As antibiotic pollution from manured farmland soils has aroused public concern, their potential interaction with manure matrix/colloids especially manure-derived dissolved organic matter (DOM) often complicated their leaching behavior. This study investigated the leaching of sulfadiazine (SDZ), and florfenicol (FFC) in undisturbed field lysimeters of chickens-integrated orchard farmland under continuous natural rainfall events. Repacked column experiments were also conducted with manure-DOM treatments under soil matrix flow. The results indicate that manure presence could reduce SDZ mass flux, but the real-time migration may increase under favorable soil hydrological processes and heavy rainfall events. Whereas FFC was more prone to leaching in manured plot (0.48 μg m^{-2} h^{-1}) as compared to the control (0.12 μg m^{-2} h^{-1}), suggesting manure-DOM facilitated FFC leaching in field via a cotransport mechanism favored by abundant macropore flow in the soil. In contrast, SDZ and FFC's mobility was reduced in repacked columns under manure-DOM conditions, suggesting increased adsorption, complexation and straining effects in soil matrix pores. Two kinetic site model and two-site nonequilibrium adsorption model fitted the breakthrough curves of SDZ and FFC well (0.988> r^2 > 0.995 for SDZ and 0.973> r^2 > 0.989 for FFC), revealing non-equilibrium conditions and kinetic sorption process in the repacked column. FFC exhibits lower leaching potential compared to SDZ in both column and field trials. Redundancy analyses revealed close relationship of FFC with humic-like components (C1 and C3), but SDZ is more related to protein-like component (C2) of manure-DOM. Therefore, as manure-DOM has a potential of increasing adsorption of highly mobile antibiotics on soil surface, however, scenario of macroporous soil under heavy rainfalls still leads to accelerated leaching. These findings highlight the combined impacts of manure-DOM and soil hydrological processes in modulating the ecological risks of antibiotics under natural conditions.

Highlights

1. Chicken manure and/or manure-DOM reduce antibiotics leaching in soil matrix flow
2. Soil macropore flow negates manure-DOM effect on antibiotics leaching in rainfalls
3. DOM PARAFAC components explain dynamic mass flux of florfenicol and sulfadiazine
4. Sulfadiazine exhibits a higher leaching potential compared to florfenicol
5. Repacked columns underestimate antibiotics leaching and ecological risk in field

1. Introduction

Veterinary antibiotics are widely used in animal husbandry to treat diseases and promote livestock productivity. Globally, China is the largest producer and user of veterinary antibiotics (Boeckel et al. 2015; Krishnasamy et al. 2015), and a large proportion are used in swine, cattle and poultry production (Chen et al. 2012; Zhao et al. 2010). Recently, it is suggested that the growth rate of poultry meat production in China may exceed pork production with 18.9 Mt of poultry meat produced in 2016 and an average of 7.2% annual increase in egg production (Wu 2019). Thus antibiotic used for chickens production is predicted to increase by 143% from 2010 to 2030 (Boeckel et al. 2015). The main concern over extensive consumption

is that veterinary antibiotics are not entirely adsorbed or metabolized *in vivo*; approximately 30–90% may be excreted as active compounds via animal urine and feces and subsequently enter into the environment (Sarmah et al. 2006; Qiao et al. 2012).

The excreted antibiotics in manure and other animal waste may be introduced into the agricultural soil through different pathways, including land application, direct excretion (grazing animals or free-ranging chicken in integrated farming systems) and wastewater (Zhao et al. 2010; Jechalke et al. 2014). After reaching the soil, these antibiotics may be leached or transported to water bodies (Kay et al. 2004; Li et al. 2015; Pan and Chu 2016; Yi et al. 2019). Antibiotic contamination can cause ecological disturbance and risks to human health (Hu et al. 2010) via the development and spread of antibiotic resistance genes in the ecological environment (Chen et al. 2014; Joy et al. 2013; Song and Guo 2014). Studies have reported extensive veterinary antibiotics contaminations in agricultural soils,urface water and groundwater systems associated with various hydrological mechanisms, mainly surface runoff and leaching from contaminated sites (Chen et al. 2017; Sun et al. 2017; Tong et al. 2017; Danner et al. 2019).

Among the key processes that remobilize contaminants in agricultural soil, leaching is important for the downward migration of veterinary antibiotics, especially for weakly sorbing antibiotics species (Kay et al. 2005; Pan and Chu 2017). Growing evidence suggests that extensive presence of manure particles, dissolved organic matter (DOM), and other associated organic colloids may alter the fate and transport potentials of veterinary antibiotics in the environment (Fan et al. 2021; Xing et al. 2020; Zhang et al. 2012; Zhou et al. 2016; Zou and Zheng 2013). Vertical migration of veterinary drugs increases the vulnerability of groundwater to pollution danger, and this could be more significant in macroporous soils dominated by preferential flow paths (Burke et al. 2016; Boy-Roura et al. 2018). However, leaching studies of veterinary antibiotics on field sites are limited. The few available studies only reported concentration data lacking sufficient information for downgradient risk assessment. Measuring concentration data concurrently with the Darcy velocity of infiltrating water (mass flux) during rainfall events is crucial for regulatory decisions and to circumvent the uncertainty associated with mass flux estimates and laboratory simulations. Nevertheless, studies on antibiotics vertical mass flux in natural field site under integrated farming system is still missing.

The potentials of manure particles and/or manure dissolved organic matter (DOM) to mediate the leaching of veterinary antibiotics has been reported in the literature (Gbadegesin et al. 2022; Lei et al. 2014; Zhou et al. 2016; Zou & Zheng 2013). DOM can constrain the partitioning, adsorption-desorption, and other key processes that influence the leaching potential of veterinary antibiotics through several physical and chemical interaction mechanisms such as complexation reaction, electrostatic interaction, van der Waals force, and hydrophobic partitioning (Bai et al. 2017; Lei et al. 2014; Lou et al. 2018; Xu et al. 2016). Albeit, a systematic investigation of this issue that reconciles field and laboratory leaching data are currently not available. The potential risk of veterinary antibiotic pollution from manured agricultural farmland requires adequate attention. Therefore, tracking DOM and its optical properties alongside the mass flux of veterinary antibiotics will provide better insights for risk management.

Sulfonamides (sulfadiazine) and chloramphenicol (florfenicol) are important classes of most consumed veterinary medicines (Fig. S1) in animal husbandry (Thiele-Bruhn 2003; Xiao et al. 2014) and are often reported to interact with DOM in the soil-water system as biologically active compounds (Lou et al. 2018; Yang et al. 2020; Zhao et al. 2019). Understanding the mass flux of these antibiotics and the coupling effects of natural field environments in association with manure DOM under rainfall conditions is essential to prevent antibiotics pollutions risks and its potential health hazards. In this light, the objectives of this study were: (1) to monitor the vertical mass flux of florfenicol (FFC) and sulfadiazine (SDZ) during natural rainfall events in orchard field integrated with free-ranging chickens (2) to explore the relationship of the antibiotics mass flux with the leachate suspended particles and the manure-DOM species as characterized using optical indices, and (3) to compare the leaching behavior in association of manure-DOM under matrix flow and field conditions.

2. Materials And Methods

2.1 Chemicals and reagents

Sulfadiazine (SDZ, $C_{10}H_{10}N_4O_2S$, CAS-Nr. 68-35-9) and florfenicol (FFC, $C_{12}H_{14}Cl_2FNO_4S$, CAS-Nr. 73231-34-2) with > 99% purity was purchased from Dr. Ehrenstorfer GmbH (Augsburg, Germany). Stock solutions (1 g L^{-1}) of both antibiotics were prepared in HPLC grade MeOH (Merck, Belgium) and finally diluted to 20 L for orchard plot spiking using tap water to obtain a final concentration of 0.05 mg mL^{-1}. High purity reagents used for Liquid chromatography-mass spectrometry (UPLC-MS/MS) analysis were purchased from Sinopharm Chemical Reagent Co., Ltd. (Shanghai, China). Isotope-labeled internal standards used to compensate for antibiotics loss during preparation and matrix effect were purchased from Toronto Research Chemicals (Berlin, Germany). Oasis hydrophilic-lipophilic balance (HLB) cartridges (6 mL 200 mg) were purchased from Waters (Milford, MA). Glass fibre filters (pore size, 0.22 µm) were purchased from Whatman (Maidstone, England).

2.2 Study site and experimental setup

The study was conducted in a small agricultural catchment in the hilly area of central Sichuan, southwestern China. The orchard plots are located as: A (105° 27' 30" E, 31° 16' 8" N), B (105° 27' 30" E, 31° 16' 9" N); and C (105° 27' 30" E, 31° 16' 9" N) at 420 m above sea level (Fig. 1). Crop farmlands account for approximately 55% of the area. The region falls under moderate subtropical monsoon climate with an annual average temperature and rainfall of 17.3°C and 826 mm (1981–2006). The maximum precipitation (65–85%) occurs in summer and autumn. The region is dominated by loamy soil, locally referred to as purple soil (an Entisol in USDA Taxonomy), and the soil is the major agricultural soil of the Upper Yangtze River, China. The soil profile consists of three layers: readily erodible topsoil (extending from 0–30 cm at the upslope and to 60 cm depth at the downslope), followed by a middle layer of fractured mudrock (with a depth of 2.1 m to 4.8 m) and the third layer is composed of impermeable sandstone.

In this study, three plots named A, B and C (122.08 m^2 surface area each) were demarcated with wire gauze in orchard farmland integrated with free-ranging chicken, a well-known traditional agricultural land use in the hilly area of central Sichuan, southwestern China. Plot A is the control (without roaming chicken), while plots B and C houses the ranging chicken. Undisturbed field soil lysimeters (50 cm width, 50 cm length, 50 cm depth, and surface area 0.25 m^2) were technically excavated and reinstalled at the center of each plot years preceding the study. The lysimeter bottom boundary was underlain with quartz sand to prevent soil sliding and blocking of the leachate collection furrow, and the leachate was channeled with an aluminum pipe into a tipping bucket rain gauge to quantify the leachate amount. Tensiometers (T4e, UMS, München, Germany) were installed at 10 cm and 30 cm depth inside the lysimeter and the open plots to monitor the water potential during rainfall events.

Table 1
Rainfall and leachate properties

Rainfall events	Rainfall amount	Duration	Maximum intensity	Preceded dry days	Average leachate discharge per 15 min (cm^3 h^{-1})		
	(mm)	(h)	(mm/15 min)	(days)	Plot A	Plot B	Plot C
8/12/2020	17.2	4	32.8	3	68.13	165.31	4.06
8/13/2020	46.6	17	28.8	1	104.06	89.14	28.75
8/15/2020	16	5	22.4	2	145.50	226	35
8/18/2020	20.2	11	12	3	77.73	190.91	51.59
Note: Plot A is the control (without manure), plot B and C represent manured plots (chicken raising orchard plots)							

In order to control interferences of residual antibiotics in the orchard farmland experiment, our target antibiotics were excluded from the medications administered to the orchard free-ranging chicken over the farming season preceding the study. Following that, 20 L of 0.05 mg mL^{-1} target antibiotics solution was sprayed evenly over each experimental plot (A, B and C) area, and the lysimeter leachates were collected under four heavy rainfall events in summer of 2020 (Table 1).

2.3 Sampling and data collection

2.3.1 Rainfall events and field lysimeter leachate

A total of four rainfall events (on the 12th, 13th, 15^{th,} and 18th of August 2020) that generated subsurface flow were monitored in this study. The lysimeter leachate was measured continuously with a tipping bucket connected to a HOBO event data logger (Onset Computer Corp., MA, USA), and the soil water potential was recorded with tensiometers (T4e, UMS, München, Germany). The rainfall amount and duration were also recorded. All data were recorded at 15 minutes intervals, and after each rainfall event, lysimeter leachate was thoroughly mixed before being sampled (Table 1).

The first three events were characteristics heavy rainfall events commonly experience in the region, while the 4th rainfall event can be classified as medium. The lysimeter discharge responded well to each rainfall events, however varied among the plots with plot C having the lowest discharge rate across all the four events monitored. The heavy event on 12th August occurred at a short duration but higher intensity after three preceding dry days, which resulted in less percolation and generated low subsurface flow, especially in plot A and C with discharge of 68.13 $cm^3\ h^{-1}$ and 4.06 $cm^3\ h^{-1}$, respectively. This is was associated to longer dry periods that cause changes in surface soil structure, especially in light-textured soils as purple soil which may alter rainfall infiltration and increase runoff generation. The subsequent events on 13th and 15th of August generated higher discharge rate of 28.75-104.06 and 35-145.50 $cm^3\ h^{-1}$. It is worthy to note the high leachate discharge rate obtained under the rainfall event on 15th of August despite its short duration, this may be connected to high antecedent water content in the soil profile which might have smoothened the pathway for preferential discharge. Earlier report show some wide differences in stream discharges rates at various locations under similar rainfall events (Dong et al. 2021). It is suggested that rainfall intensity, duration and the numbers of antecedent dry days may influence the lysimeter discharge rate and amount.

2.3.2 Chicken manure-DOM extraction and column experiments

Manure DOM was extracted from chicken manure (Table 2) by shaking method. Briefly, fresh chicken manure sample was air-dried, sieved with a 60-mesh sieve, and extracted with 0.01 mol L^{-1} $CaCl_2$ and 0.1 g L^{-1} NaN_3 solution in a 50 mL plastic centrifuge tube. The mixture was shaken at 180 r min^{-1} at 25 ℃, for 16 h, sonicated for 30 min, centrifuge at 25℃, 8000 r min^{-1} for 10 min, and finally filtered using 0.45 μm PTFE filter membrane to obtain water-extractable manure DOM.

The effects of chicken manure-DOM on SDZ and FFC leaching behavior in purple soil was further examined in repacked soil columns under saturated conditions. Composite soil samples were collected from the experimental plot (Table 2), air-dried, sieved (2 mm), and treated differingly with chicken manure-DOM (Haham et al. 2012). The effects of DOM on VAs leaching was examined in two ways: (i) leaching in column loaded with DOM pre-coated soil (pre-equilibrated with 100 mg OC/L DOM for 4 days) and (ii) sieved soil samples (Haham et al. 2012).

Table 2
Selected properties of the orchard soil and chicken manure

Samples	Sand	Texture		pH	OC	DOC	CEC	ρ
		Silt	Clay		(g kg^{-1})	(mg L^{-1})	(cmol kg^{-1})	(g cm^{-3})
Orchard soil	30%	66%	4%	7.98	15.52	38.2	18.2	1.49
Chicken manure	ND	ND	ND	7.28	486.25	7977	53.41	ND

Note: OC organic carbon, DOC dissolved organic carbon, CEC cation exchange capacity, ρ bulk density, ND not determined.

Columns (15 cm length, 1.25 cm in inner diameter) were packed at 1 cm increments by gradual tapping with a pestle to ensure uniform packing. Our pre-experiment confirmed that SDZ and FFC sorption onto the column wall is negligible. The soil columns bulk density and porosity range from 1.43–1.49 g cm-3, and 0.44–0.46, respectively. All columns were slowly saturated from the bottom with a solution of 0.1 g L^{-1} NaN_3 and 0.01 mol L^{-1} $CaCl_2$ at a flow rate of 20.3 µL min^{-1} for approximately 48 h at a steady flow rate before being injected with 5 pore volumes (PV) of the solution containing the target antibiotics in combination of manure DOM and nonreactive tracer (1 mg L^{-1} VAs + 100 mg L^{-1} DOM + 100 mg L^{-1} Br -) at a flow rate of 162.5 µL min^{-1} (equivalent to 21.7 mm h^{-1} rainfall), and finally eluted with 4 PV of background solution (0.1g L^{-1} NaN_3 and 0.01 mol L^{-1} $CaCl_2$).

2.4 Analyses

2.4.1 Sample analysis

The target antibiotics (SDZ and FFC) in lysimeter leachate were analyzed using high-performance liquid chromatography-tandem mass spectrometry (Framingham, Massachusetts, USA). The analytical column consists of a BEH C18 column (2.1×100 mm, 1.7 µm, Waters, Milford, Massachusetts, USA). Lysimeter leachate (2 L) were acidified, filtered through a 0.45 mm PES membrane (Millipore, Billerica, MA), and isotopic standards were added before being loaded into a pre-conditioned Oasis HLB cartridge.

Some selected parameters, including pH, EC, DOC, colloid concentration, and particles size distribution (PSD), were measured within 24 h after sampling. The pH was measured with pH meter (Leici Environmental Co, Shanghai, China), colloid concentration was determined after 2 min of ultrasound (100 W) in water bath sonicate (KQ-3000VDE, Huqin Equipment Co., Ltd., Shanghai, China) by spectrophotometer (Tu-1810, Purkinje General Instrument Co., Beijing, China). Distribution of particles in lysimeter leachate was measure by laser scattering particle size distribution analyzer (LA950, Horiba, Kyoto, Japan), and DOC was measure by TOC analyzer (OI Analytical Aurora 1030C, USA).

Further, the UV-visible absorbance (200 to 600 nm) and excitation-emission matrix (EEM) fluorescence (at emission wavelengths from 250–800 nm and excitation wavelength from 240 to 600 nm) of the lysimeter leachate was obtained by an Aqualog fluorescence spectrometer (Horiba JY Aqualog, Japan) at 1 nm

increments and an integration time of 0.5 s. The results were corrected for Inner-filter effects, Raman bands, and Rayleigh scatters, and instrument-specific spectral biases were removed. The spectral peaks were investigated using parallel factor (PARAFAC) analysis (Stedmon and Bro 2008). Optical indices were calculated to describe the compositional characteristics of the leachate DOM: (1) $SUVA_{254}$ describe aromaticity of DOM and it is the ratio of UV absorbance at 254 nm (m^{-1}) and DOC concentration (mg-C L^{-1}), (2) fluorescence index (FI) reflects the contribution of microbial (> 1.9) and plant (< 1.4), and it was calculated as the ratio of the emission intensity at 470 nm and 520 nm at an excitation of 370 nm (Cory and McKnight 2005); and (3) humification index (HIX) was calculated as the ratio of the peak integrated area from 435 to 480 nm and the sum of the emission spectra over 300–345 nm and 435–480 nm at an excitation of 254 nm (Ohno 2002).

2.4.2 Mass flux of SDZ and FFC

Mathematically, the mass flux (J) of the target antibiotics passing through the cross-sectional area of the undisturbed field lysimeter (50×50×50 cm) in orchard-chicken integrated farmland during rainfall can be calculated as follows:

$$J = qC$$

1

$$q = -K\frac{\partial h}{\partial z}$$

2

Where J is the mass flux [$ML^{-2}T^{-1}$], q is Darcy flux [LT^{-1}] calculated using the tipping bucket leachate flow data recorded at 15 min interval, C antibiotics concentration in the liquid phase [ML^{-3}], K is hydraulic conductivity [LT^{-1}], $\partial h/\partial z$ is the hydraulic gradient [dimensionless].

2.5 Modelling

2.5.1 One-dimensional transport and sorption parameters

A convection-dispersion equation for one-dimensional transport behaviour of the target antibiotics in repacked soil column were fitted with HYDRUS-1D (Simunek et al. 2008) based on two concept (1) two kinetic retention sites and (2) two sites chemical nonequilibrium adsorption model (Selim et al. 1976; van Genuchten and Wagenet 1989) with Freundlich adsorption isotherm were implemented in this study.

2.5.2 Two-site nonequilibrium adsorption model

This model conceptually divided the sorption sites into two fractions. It assumes that adsorption on Type 1 sites is instantaneous while adsorption on the other fraction (Type 2 sties) is kinetically controlled (van Genuchten and Wagenet 1989; Šimůnek et al. 2013):

$$S = S^{e} + S^{k}$$

3

where S^e and S^k [M M^{-1}] are fractions of the sorption sites assumed to be instantaneous [Type 1] and first-order kinetic rate [Type 2], respectively.

Thus, the conventional advection-dispersion equation is modified as follows:

$$\frac{\partial c}{\partial t} + \rho\frac{\partial S^e}{\partial t} + \rho\frac{\partial S^{\mathrm{k}}}{\partial t} = \frac{\partial}{\partial z}\left(\theta D\frac{\partial c}{\partial z}\right) - \frac{\partial qc}{\partial z} - \varphi$$

4

$$S^{\mathrm{e}} = f_{\mathrm{e}}K_f C^{\square}$$

5

$$\rho\frac{\partial S^{\mathrm{k}}}{\partial t} = \alpha_{\mathrm{k}}\rho(S_{\mathrm{e}}^{\mathrm{k}} - S^{\mathrm{k}}) - \varphi_{\mathrm{k}}$$

6

$$S_{\mathrm{e}}^{\mathrm{k}} = \alpha_{\mathrm{k}}\left(1 - f_{\mathrm{e}}\right)K_f C^{\square}$$

7

The bromide BTC was fitted to obtain dispersivity λ (cm): $\lambda = D/v$ (8)

where ρ is the porosity [L^3 L^{-3}]; t is time [T]; c is the solution concentration [M L^{-3}]; S^e *and* S^k is the sorbed concentration on equilibrium and kinetic sorption sites [M M^{-1}], respectively; θ is the water content [L^3 L^{-3}]; D is the hydrodynamic dispersion coefficient [L^{-2} T^{-1}]; λ is dispersivity, v pore velocity, z is the depth [L]; $\rho$is the bulk density [M L^{-3}]; f_e is the fraction of sorption sites in equilibrium with liquid-phase (dimensionless), K_f is the Freundlich distribution coefficient ($M^{1-\square}L^{3\square}M^{-1}$), $\square$ s the dimensionless Freundlich exponent, α_k is the first-order rate coefficient associated with the kinetic site (T^{-1}), and φ is the sink term [n L^{-3} T^{-1}], v is the average pore water velocity (cm min^{-1}).

2.5.3 Two kinetic site model

The two kinetic site model (Eq. 9–11) assumes that adsorption occur kinetically on both fractions of the sorption sites and proceed at different rates, which can be written as:

$$\frac{\partial c}{\partial t} + \rho\frac{\partial S_1^{\mathrm{k}}}{\partial t} + \rho\frac{\partial S_2^{\mathrm{k}}}{\partial t} = \frac{\partial}{\partial z}\left(\theta D\frac{\partial c}{\partial z}\right) - \frac{\partial qc}{\partial z} - \varphi$$

9

$$\rho \frac{\partial S_1^{\mathrm{k}}}{\partial t} = k_{\mathrm{a1}} \theta c - k_{\mathrm{d1}} \rho S_1^{\mathrm{k}} - \varphi_{\mathrm{k1}}$$

10

$$\rho \frac{\partial S_2^{\mathrm{k}}}{\partial t} = k_{\mathrm{a2}} \theta c - k_{\mathrm{d2}} \rho S_2^{\mathrm{k}} - \varphi_{\mathrm{k2}}$$

11

Where ∂S_1^k and ∂S_2^k are the sorbed concentration of the first and second kinetic sorption sites [M M^{-1}], respectively; k_{a1} and k_{a2} are the attachment coefficients of the first and second fraction of kinetic sorption sites [T^{-1}], respectively; k_{d1} and k_{d2} are the detachment coefficients of the first and second fraction of kinetic sorption sites [T^{-1}], respectively; ϕ_{k1} and ϕ_{k2} are the sink term for the first and second kinetic sorption that represent various reactions at the kinetic sorption sites [n L^{-3} T^{-1}].

3. Data Analysis

The mass flux of the target antibiotics with lysimeter leachate was calculated (Eq. 1–2). Statical analyses were conducted using one-way ANOVA to compare the mass flux of the two antibiotics (SDZ and FFC). Significant differences were considered at a $p < 0.05$. DOM optical properties were investigated using fluorescence excitation-emission matrix coupled with parallel factor analysis (EEM-PARAFAC). DOM Redundancy analysis was performed to evaluate the relationship between EEM-PARAFAC components, DOM and its optical indexes, suspended particle, and mass flux of the target antibiotics.

4. Results And Discussion

4.1 Soil flow dynamics corresponding to natural rainfall events

Soil water potential is usually used to infer the soil water movement, and it is a valuable tool for understanding antibiotics mass flux in macroporous soil. The water potential of the three experimental plots (A, B and C) continuously monitored during the four-rainfall events (Table 1) showed that the lysimeters soil profile were saturated during the rainfall events (Fig. 2) as recorded at 10 cm and 30 cm profile depth (water potential > 0 cm). During the first rainfall event (12th

August 2020) with the highest maximum intensity (32.8 mm/h) but short duration (4 h), the water potential indicated consistent soil water penetration into the lysimeter soil profile depth. The trend in control plot A showed earlier and higher saturation at the lower soil depth (30 cm) than the upper soil depth (10 cm depth). Interestingly, the two observation depths (10 cm and 30 cm) indicated a similar soil water response to the rainfall event. Similar trends of soil water potentials were observed in chicken-integrated plots (B and C) at two observation depths (10 cm and 30 cm), which were almost overlapping.

The second rainfall event came after 24 h with a lower maximum intensity (28.8 mm/h) but longer duration (17 h). During the rainfall event, the soil profile wetting followed a similar pattern as was observed during rainfall event I. It is worthy to note the consistently high-water saturation level at the lower soil depth (30 cm depth) than the upper depth (10 cm depth) in control plots A under each of the four rainfall events monitored. Manured plot B also indicated this scenario during events 1 and 3 and manured plot C during events 3 and 4 (Fig. 2). Earlier and higher saturation levels of the lower soil depth suggest that the infiltrating water may have bypassed the upper soil profile to saturate the lower depth through preferential flow channels.

The water potential measured in the open field within the experimental plot suggests that the lysimeter soil profile was more saturated than the open field at the two observation depths, especially in control plots A and manured plot B, as showed by positive water potential values (Fig. S2 of the SI). For instance, the lower depth (30 cm) in the open field soil profile (at 30 cm depth) in plots A and B does not attain full saturation (water potential ranges from − 20 to 30 cm), possibly due to continuously lateral flow in the interconnected pore present in the wide-open plot condition. Interconnected pore networks may permit lateral water transmission compared to the lysimeter soil profile with narrow surface area and restricted lysimeter walls where vertical flow may dominate. However, the water potential at 10 cm and 30 cm depth in the open field condition of manured plot C were more saturated than the lysimeter soil profile depths. Overall, soil water movement and saturation inside the lysimeter soil profile and the open field were similar, as suggested by water potential trend during the events. The earlier and higher water saturation scenario at the lower soil profile depth (30 cm depth) than the upper profile (10 cm depth) was also observed at the open field profile. This may be due to the abundance of rapid subsurface flow channels associated with root holes, wormholes, interaggregate pore spaces, and preferential flow channels peculiar to macroporous soils. This phenomenon has been reported in previous studies conducted at a different location in the same study site (Zhao et al. 2013; Zhang et al. 2015). Subsurface flow is the main pathway for contaminant transport in the region, accounting for over 88% of runoff. As earlier reported the saturated hydraulic conductivity (Ks) of the region ranged from 37–43 mm h^{-1} (for 10–15 cm depth) (Wang 2013), while 17.6 mm h^{-1} (for 25–30 cm depth) and 12.9 mm h^{-1} were reported for the fractured mudrock region (Zhang et al. 2016). The subsurface soil is characterized by large structuralores (> 0.21 cm^3 cm^{-3}) for water movement, and large pores (> 250 μm) usually account for above 90% of the Ks. As such, the hydrological condition of the region influences the water quality status of the Yangtze River. Overall, the considerably varied water potential observed in the lysimeter soil profile of three plots (A, B and C) suggests soil pore distribution heterogeneity in field conditions. More importantly, the effects of disconnected lateral flow paths caused by the restricting lysimeter wall are complex irrepressible scenarios in natural field sites.

4.2 Mass flux of sulfadiazine and florfenicol in lysimeter leachate

The mean overall mass flux of SDZ and FFC in lysimeter leachate under the four rainfall events observed are shown in Fig.3. SDZ showed significantly higher leaching and migration potential (ranging from 2.7 to

6.6 μg m^{-2} h^{-1}) compared to FFC across the three plots (Plots A, B and C). The mass flux of SDZ (4.2 and 2.7 μg m^{-2} h^{-1} in plots B and C, respectively) chicken manured plot B was considerably lower compared to 6.6 μg m^{-2} h^{-1} in control plot A. High leaching potential of SDZ to groundwater has been reported in the literature (Engelhardt et al. 2015; Wang et al. 2015). It was also suggested that the presence of manure and/or manure-DOM may increase SDZ adsorption tendency in the soil (Sukul et al. 2008; Wang et al. 2015; Conde-Cid et al. 2019), but the retention potential in soil profile may depend on the soil hydrological processes during rainfall events.

Contrastingly, the mass flux of FFC was generally low across the orchard field plots Fig. 3. The lowest mass flux of 0.12 and 0.02 μg m^{-2} h^{-1}occurred in the control plot A (non-manured) and plot C (manured but rarely visited by the ranging chicken), respectively. While the mass flux in manured plot B was moderately higher (0.48 μg m^{-2} h^{-1}), suggesting facilitated transport of FFC in chicken manured plots. This result contradicts previous reports in column studies, where FFC mobility was reportedly reduced in manure amended soils and leached at a high mobility rate similar to nonreactive bromide tracer in the absence of manure DOM (Tang et al. 2021).

The antibiotics mass flux was further examined based on each rainfall event monitored (Fig. 4). Statistical analysis confirmed significantly higher FFC mass flux in manured plot B as compared to other plots, especially under events I, III and IV. The first rainfall event with the highest maximum intensity (32.8 mm/h) but a short duration (4 h) leads to the highest mass flux. However, the mass flux considerably reduced sequentially in succeeding rainfall events I, II and IV in the order of $1.41 > 0.18 > 0.09$ μg m^{-2} h^{-1}, respectively. Compared to manured plots, significantly higher mass flux of FFC from control plot A was only observed during rainfall event II. The recurrently higher FFC mass flux under events I, II and IV suggest possible FFC interaction with chicken manure and/or mobile manure DOM. Compared to FFC, SDZ mass flux from control plot A during rainfall events I, II and IV consistently showed significantly lower leaching flux, except under rainfall event III, where the mass flux was significantly higher than other plots. Similarly, the mass flux of SDZ in plots B and C (chicken manured) was reasonably higher than plot A (control) except during event III. It is worthy to note the decreasing mass flux of the antibiotics (especially FFC) with succeeding rainfall events observed in all plots.

Overall, SDZ showed strong leaching potentials in control plot A (non-manured plot), while FFC was more prone to leaching in chicken-manured orchard purples soil. The high mass flux of antibiotics in manured plots can be linked to possible antibiotics interaction with manure-DOM, mobile manure particles and other influencing factors of manure DOM under the influence of soil hydrological conditions.

4.3 EEM-PARAFAC components during rainfall events

The EEM-PARAFAC analysis of the lysimeter leachate for each monitored rainfall event showed that the DOM contains three main components designated as component 1 (C1) at excitation/emission (Ex/Em) wavelengths of 270(380)/430 nm, component 2 (C2) 260(400)/480 nm and component 3 (C3) 270/370 nm (Fig. 5 and Table S1 of the SI). Previous studies have classified components C1 and C2 as typical UVA

humic-like components consisting of fulvic-acid-like materials, while component C3 is a characteristic protein-like substance (Xian et al. 2018; Liu et al. 2019; Gao et al. 2020).

The distribution and the relative abundance of DOM and the identified EEM-PARAFAC components C1, C2 and C3 are shown in Fig.6. The proportion of DOC (ranges from 42–54%) and components C1 (ranges from 44–47%) in lysimeter leachate from the control plot was consistently higher than manured plots (B and C with free-ranging chicken) during the first three rainfall events (I, II and III). Interestingly, control plot A has the lowest proportion of components C2 and C3. While the leachate from plots B and C with chicken manure have a reasonably higher proportion of components C2 and C3, with C2 ranging from 16–51% and 28–73% in plots B and C, respectively. Similarly, C3 ranges from 23–53% and 15–61% for plots B and C, respectively. These results revealed that DOM concentration of the leachate samples is insufficient to understand the modulating factors of antibiotics mass flux in orchard farmlands. Thus disproportionality of PARAFAC components in the leachate samples may have important implications for the differences observed in SDZ and FFC mass flux across the studied plots.

For example, a low proportion of DOC was observed in lysimeter leachate from plot B compared to other plots plot (A and C) during rainfall event 1. Nevertheless, the corresponding mass flux of SDZ and FFC in plot B was significantly higher than in other plots despite their higher DOC values (Figs. 5 and 6). The higher mass flux of SDZ and FFC in plot B coincides with the higher proportion of components C2 and C3 observed in its leachate samples. Similarly, a higher proportion of DOC and components C1 observed in the leachate samples from control plot A may be related to the significantly higher mass flux of FFC under rainfall event II. Likewise, the high proportion of components C2 and C3 in plots A and B might be linked to the significantly higher mass flux of SDZ in their leachate. FFC mass flux was significantly higher during rainfall event III in manured plot B, followed by control plot A. This can be associated to their higher proportion of DOC and component C1, while the significantly low proportion of FFC mass flux in Plot C directly corresponds to its low DOC and C1. Similarly, during rainfall event IV, significantly higher mass flux of FFC was observed in manured plot B, which corresponds to its higher proportion of DOC and component C1. These findings suggest that PARAFAC components influence the mass flux of FFC and SDZ in our experimental plots, and the specific impact may vary depending on the distribution of the components and their interaction with antibiotics species.

4.4 Response of antibiotics mass flux to DOC and optical indices of DOM

Redundancy analysis (RDA) was conducted to better understand the specific relationship between the mass flux of FFC, SDZ and DOM optical indices (Fig.7 and Table S1 of the SI). The result showed that the combined effects of DOM optical indices and suspended particles in the lysimeter leachate, including colloids and water suspended microparticles (PSD<10 μm), accounted for 93.9% of the total variation of SDZ and FFC mass flux from orchard plots. The influencing variables C1, DOC, PSD<10 μm, and HIX accounted for 27.9%, 23.1%, 12.8%, and 12.7% of the total variation. FFC had a close relationship with C1, PSD<10 μm, and $S_{R,}$ while SDZ is more related to C2, $SUVA_{254}$ and HIX. RDA suggests that DOC and colloids may have negative impacts on SDZ mass flux. The results indicated a strong association between

the environmental variables and the mass flux of SDZ and FFC in orchard purple soil. It can be inferred that DOM with a high proportion of PARAFAC components C1 and C3 may enhance FFC mass flux in the subsurface soil, and this could be more significant in flow-channels dominated with a high proportion of water suspended microparticles < 10 μm.

These results corroborated previous studies that reported significant correlations between PARAFAC-derived DOM components and various classes of antibiotics, including sulfonamides, tetracycline, quinolones and macrolides, their occurrence and ecological risks using RDA (Mu et al. 2018; Zhang et al. 2019). Further, the results suggest that field plots with high subsurface particle transports may critically influence the leaching of antibiotics in the presence of manure under natural rainfall. Therefore, the leaching antibiotics may be strained/or adsorbed in smaller soil pores or facilitated in preferential flow channels.

4.5 FFC and SZD breakthrough curves in repacked soil column

The breakthrough curve (BTC) of nonreactive bromide tracer obtained for control and chicken manure DOM treated repacked columns showed no visible trend that could indicate incorporation of DOM affected the soil structure Fig.8. Similarly, the bromide BTCs adequately conform to the physical equilibrium model, confirming the absence of preferential flow channels in the transport domain in the repacked columns. However, the fitted dispersity (λ) obtained from bromide BTC (ranges from 0.7 and ~1.2 for control and DOM treated columns, respectively) indicated flow heterogeneity related to the packing process. These values were used to simulate SDZ and FFC transport in each column in order to account for possible variation in the flow domain.

Figure 8 showed the BTC of SDZ and FFC in columns under DOM influence. The BTC of both antibiotics in the presence and absence of manure DOM treatments were reasonably delayed relative to nonreactive bromide tracer. Bromide BTC occurred after 0.2 PV compared to SDZ, which peak appeared approximately 1.4, 1.2 and 1.4 PV in control (columns without manure DOM), and manure DOM treated columns (DOM pre-coated and non-precoated cotransport condition). The curve indicates a higher relative delay of SDZ BTC in control (without DOM) and DOM co-transport condition compared to DOM pre-coated condition. Similarly, FFC BTC was relatively delayed compared to bromide tracer. FFC BTC in control and DOM co-transport column was 1.6 PV delayed while DOM pre-coated condition leads to 1.4 PV delay. Overall, the FFC BTC showed relative delayed breakthrough tendency compared to SDZ under manure DOM treatments conditions.

Additionally, differences were further observed in the peak maxima of the antibiotics compared to bromide tracer. Despite the comparable conditions, the maximum relative concentrations (C/C_0) of SDZ and FFC BTC relative to bromide (Br) BTC were lower and varied according to various DOM treatments. The maximum C/C_0 of bromide and the antibiotics were in the order of Br (0.98) > SDZ (0.96) > FFC (0.89), Br (0.98) > SDZ (0.84) > FFC (0.81) and Br (0.98) > SDZ (0.92) > FFC (0.81), for control, DOM pre-coated and DOM co-transport treatment conditions, respectively. The lower peak maxima of the antibiotics (SDZ and

FFC) suggest reactive transport and sorbing nature of the antibiotics in the presence of manure DOM. The results aligned with previous studies that revealed delayed peak maxima of SDZ in the presence of manure while FFC leaching was enhanced in the presence of manure colloid (Wehrhan et al. 2007; Zou and Zheng 2013).

It is worthy to note that a complete breakthrough of SDZ was not achieved in control and DOM pre-coated columns within the experimental duration (48 h) as showed by the pronounced tailing Fig. 8. However, a complete breakthrough of SDZ under DOM co-transport treatment condition was achieved after 8.9 PV. It can be inferred that DOM pre-coating may increase SDZ adsorption and retardation in the soil profile. The result substantiates previous studies that reported incomplete breakthrough of SDZ after three weeks experimental duration (Wehrhan et al. 2007). Contrarily, FFC complete breakthrough was achieved in control and all DOM treatment conditions but however varied. The complete breakthrough of FFC was achieved after 7.3 PV, 7.8 PV and 8.5 PV under control, DOM pre-coated and co-transport conditions, respectively. This can be associated to the weakly hydrophobic nature of FFC, which may promote its weak adsorption and less retardation in soil (Zou and Zheng 2013).

4.5.1 Simulated SDZ and FFC breakthrough curves

The BTCs of SDZ and FFC were fitted by two different transport models (Eqs. 3–7 and Eqs. 9–11), as shown in Fig. 8 and Fig. S3. The fitted parameters, model statistics and the calculated eluted mass (EM) fractions are given in Table 3 and S2 of the SI. The eluted mass fraction of SDZ (ranges from 84%-96%) was considerably higher than FFC (ranges from 81–89%). The presence of DOM substantially reduced SDZ leaching, with DOM pre-coating technique having the most considerable impact on SDZ transport (EM of 84%), while DOM co-transport condition slightly lowered the EM fraction to 91.64%. Previous finding suggest that the transport of SDZ in the presence of manure resulted in lower peaks and slightly lower eluted mass compared to control columns without manure (Unold et al. 2009). This was associated to extensive sorption of SDZ to immobile manure particles and straining effects in the smaller soil pores dominating repacked soil column. Similar observation showed increased sorption tendency (K_D sorption ranging from 6.9 to 40.2) of SDZ in the presence of manure in several agricultural soils of various physicochemical properties (Sukul et al. 2008). Likewise, the co-transport of SDZ with manure DOM was reported to pose minor relevance to the eluted mass deficit of SDZ.

It is worthy to note that distinct physical differences were not observed for FFC BTCs under all treatment conditions because the pre-coated and co-transport DOM treatments technique equally reduced the EM fraction (< 81%). Since this study was conducted within a short duration (48 h), we assumed biodegradation is negligible. Therefore, the mass deficit observed suggest possible interactions between antibiotics-DOM-soil system such as complexation reaction, co-adsorption and hydrophobic partitioning unto immobile manure DOM particles attached to the soil matrix (strained), which all influences the leaching behaviour of antibiotics (Lei et al. 2014; Lou et al. 2018; Xu et al. 2016).

Table 3
Fitting parameters of two kinetics sorption sites model

Treatments		k_{a1} (min^{-1})	k_{a2} (min^{-1})	k_{d1} (min^{-1})	K_{d2} (min^{-1})	R^2	RMSE	EM%
SDZ	Control	4.78E-03 (± 8.70E-04)	0.36 (± 0.02)	5.24E-04 (± 8.9E-05)	1.13 (± 0.02)	0.988	5.31E-02	95.70
	Precoated	0.025725 (± 0.01)	1.55E-03 (± 2.3E-04)	4.20E-03 (± 8.8E-04)	1.15E-06 (± 6.49E-05)	0.990	1.61E-02	84.07
	Co-transport	0.033289 (± 3.7E-03)	6.07E-04 (± 2.75E-05)	1.16E-06 (± 3.20E-05)	6.58E-04 (± 1.60E-05)	0.995	1.21E-02	91.64
FFC	Control	8.35E-04 (± 3.18E-05)	0.16 (± 0.06)	3.36E-05 (± 1.18E-04)	0.32491 (± 2.9E-03)	0.973	7.87E-02	89.21
	Precoated	0.03 (± 4.00E-03)	1.28E-03 (± 8.99E-05)	3.46E-04 (± 7.98E-05)	1.23E-05 (± 5.29E-05)	0.987	1.85E-02	81.32
	Co-transport	0.05 (± 4.95E-03)	1.73E-03 (± 9.83E-05)	9.46E-06 (± 2.61E-5)	3.16E-04 (± 3.02E-05)	0.989	3.73E-02	81.13

Note: k_{a1} is the first-order retention coefficient on Type 1 site, k_{d1} is the first-order detachment coefficient on Type 1 site, k_{a2} is the first-order detachment coefficient on Type 2 site, k_{d1} is the first-order detachment coefficient on Type 2 site R^2 coefficient of determination. RMSE is the root mean square error. 95% confidence intervals are given in brackets.

The model statistics (Tables 3 and S2 of the SI) showed that the BTCs of SDZ and FFC were best represented by the two models (TSM and TKS model) as indicated by the coefficient of determination (R^2) ranging from 0.988–0.995 and 0.973–0.989 for SDZ and FFC, respectively, and low root mean square error (RMSE). Although the maximum peak concentration of SDZ under DOM pre-coated treatment was vastly overestimated by the TSM model Fig. S3 (a), except the rising and decreasing limbs of the BTC that was reasonably well fitted. The fitted TSM-Freundlich sorption model parameter of SDZ showed that the fraction of adsorption sites responsible for instantaneous sorption (*f)* decreased in the presence of DOM from 0.30 *f* values in control to 0.09 and 0.13 for DOM pre-coated and co-transport conditions, respectively. At the same time, the *f* value for FFC was increased from 0.06 (control) to 0.10 and 0.22 for DOM pre-coated and co-transport conditions, respectively. Similarly, Table S2 showed that the fitted Freundlich adsorption constant (K_f) reasonably increased in the presence of DOM from 0.63 to 2.93 and

8.29 for SDZ and from 9.74 to 13.04 and 33.19 for FFC. These results indicate the occurrence of irreversible antibiotics sorption during leaching simulation in the repacked soil columns and demonstrate the reason for the low EM fractions observed.

The fitted TKS model parameters (Table 3) also indicated that the presence of DOM increased antibiotics attachment rate to site 1 (k_{a1}) and decreased the attachment rate to site 2 (k_{a2}), while the corresponding detachment rates on both kinetic sites (k_{d1} and k_{d2}) were reduced. The results further explain the reason for the incomplete elution and increased K_f values observed in the presence of manure DOM. Furthermore, the optimized kinetic sorption rate coefficient (α) of SDZ and FFC was decreased in the presence of manure DOM and stayed approximately stable (Table 3). The decrease of α values during SDZ and FFC leaching in repacked columns in the presence of manure DOM implies reduced mobility of the antibiotics in the column.

5. Conclusion

Different observations were obtained from on-site lysimeter and laboratory column test. Field monitoring indicates a significant increase in SDZ leaching for the manure treatment than the control under natural rainfalls. Further evidence revealed manure colloidal DOM-facilitated transport as indicated by strong correlations of SDZ with DOM PARAFAC component C2. Characteristic preferential flow channels validated in this study is believed to have provided a major pathway for the high SDZ mass flux in manured plots. The mass flux of FFC was lower compared to SDZ under all treatment conditions but leached in a similar mechanism with manure impact. In contrast, the presence of chicken manure leads to lower peak maxima and reduced elution of both antibiotics in repacked soil columns. This clearly indicates increased retardation and sorption of antibiotics in the soil matrix, probably due to manure-colloidal bounding interactions in matrix pores. Two kinetic sites (TKS) model best fitted the antibiotics' BTCs. Meanwhile, two-site nonequilibrium adsorption model (TSM) coupled with Freundlich sorption isotherm also provided a valuable description. The fitted parameters from both models strongly supported our observations. Therefore, interaction of SDZ and FFC with chicken manure and/or manure DOM may aggravate their leaching potentials in macroporous soils dominated by abundant preferential flow channels. Nevertheless, scenario in matrix soil may lead to substantial retardation and irreversible sorption. This study provides a significant basis for evaluating the environmental risk of antibiotics leaching associated with manure-DOM impact.

Declarations

Authors' contributions Lanre Anthony Gbadegesin contributed to the field sampling and analysis, the collection and processing of experimental data, and the drafting of this manuscript. Xinyu Liu participated in the investigation, interpretation of experimental data and the preparation of this manuscript. Dr. Chen Liu was in charge of supervising all experimental and interpretative activities, funding acquisition, editing and completing the final version of the manuscript. Prof. Xiangyu Tang supervised the writing-review and editing of the manuscript. All of the authors read and approved the final manuscript.

Funding This study was supported by the National Natural Science Foundation of China (41771521) and the Youth Innovation Promotion Association, Chinese Academy of Sciences. The authors also appreciate the support from CAS-TWAS President's Fellowship for international PhD students.

Data availability The datasets used and/or analyzed during this study are available from the corresponding author on reasonable request.

Ethical approval and consent to participants Not applicable.

Consent for publication Not applicable.

Conflict of interests The authors declare no competing interests.

References

1. Bai L, Cao C, Wang CC, Wang CC, Zhang H, Jiang H (2017) Roles of phytoplankton- and macrophyte-derived dissolved organic matter in sulfamethazine adsorption on goethite. Environ Pollut 230:87–95. https://doi.org/10.1016/j.envpol.2017.06.032
2. Van Boeckel TP, Brower C, Gilbert M, Grenfell BT, Levin SA (2015) Global trends in antimicrobial use in food animals. Proceedngs Natl Acad Sci USA 112:5649–5654. https://doi.org/10.1073/pnas.1503141112
3. Boy-Roura M, Mas-Pla J, Petrovic M, Gros M, Soler D, Brusi D, Menció D (2018) Towards the understanding of antibiotic occurrence and transport in groundwater: Findings from the Baix Fluvià alluvial aquifer (NE Catalonia, Spain). Sci Total Environ 612:1387–1406. https://doi.org/10.1016/J.SCITOTENV.2017.09.012
4. Burke V, Richter D, Greskowiak J, Mehrtens A, Schulz L, Massmann G (2016) Occurrence of antibiotics in surface and groundwater of a drinking water catchment area in Germany. Water Environ Res 88:652–659. https://doi.org/10.2175/106143016X14609975746604
5. Chen C, Li J, Chen P, Ding R, Zhang P, Li X (2014) Occurrence of antibiotics and antibiotic resistances in soils from wastewater irrigation areas in Beijing and Tianjin, China. Environ Pollut 193:94–101. https://doi.org/10.1016/j.envpol.2014.06.005
6. Chen L, Lang H, Liu F, Jin S, Yan T (2017) Presence of antibiotics in shallow groundwater in the northern and southwestern regions of China. Groundwater 6:451–457. https://doi.org/10.1111/gwat.12596
7. Chen YS, Zhang HB, Luo YM, Song J (2012) Occurrence and assessment of veterinary antibiotics in swine manures: A case study in East China. Chin Sci Bull 57:606–614. https://doi.org/10.1007/s11434-011-4830-3
8. Conde-Cid M, Fernández-Calviño D, Fernández-Sanjurjo MJ, Núñez-Delgado A, Álvarez-Rodríguez E, Arias-Estévez M (2019) Adsorption/desorption and transport of sulfadiazine, sulfachloropyridazine, and sulfamethazine, in acid agricultural soils. Chemosphere 234:978–986. https://doi.org/10.1016/j.chemosphere.2019.06.121

9. Cory RM, McKnight DM (2005) Fluorescence spectroscopy reveals ubiquitous presence of oxidized and reduced quinones in dissolved organic matter. Environ Sci Technol 39:8142–8149
10. Danner MC, Robertson A, Behrends V, Reiss J (2019) Antibiotic pollution in surface fresh waters: Occurrence and effects. Sci Total Environ 664:793–804. https://doi.org/10.1016/j.scitotenv.2019.01.406
11. Dong J, Xie H, Feng R, Lai X, Duan H, Xu L, Xia X (2021) Transport and fate of antibiotics in a typical aqua-agricultural catchment explained by rainfall events: Implications for catchment management. J Environ Manage 293:112953. doi: 10.1016/j.jenvman.2021.112953
12. Engelhardt I, Sittig S, Šimůnek J, Groeneweg J, Pütz T, Vereecken H (2015) Fate of the antibiotic sulfadiazine in natural soils: Experimental and numerical investigations. J Contam Hydrol 177–178:30–42. https://doi.org/10.1016/j.jconhyd.2015.02.006
13. Gao J, Shi Z, Wu H, Lv J (2020) Fluorescent characteristics of dissolved organic matter released from biochar and paddy soil incorporated with biochar. RSC Adv 10:5785–5793. https://doi.org/10.1039/c9ra10279e
14. Gbadegesin LA, Tang X, Liu C, Cheng J (2022) Transport of veterinary antibiotics in farmland soil: Effects of dissolved organic matter. Int J Environ Res Public Health 19:1702. doi: 10.3390/ijerph19031702
15. Haham H, Oren A, Chefetz B (2012) Insight into the role of dissolved organic matter in sorption of sulfapyridine by semiarid soils. Environ Sci Technol 46:11870–11877
16. Hu X, Zhou Q, Luo Y (2010) Occurrence and source analysis of typical veterinary antibiotics in manure, soil, vegetables and groundwater from organic vegetable bases, northern China. Environ Pollut 158:2992–2998. https://doi.org/10.1016/j.envpol.2010.05.023
17. Jechalke S, Heuer H, Siemens J, Amelung W, Smalla K (2014) Fate and effects of veterinary antibiotics in soil. Trends Microbiol 22:536–545. https://doi.org/10.1016/j.tim.2014.05.005
18. Joy SR, Bartelt-Hunt SL, Snow DD et al (2013) Fate and transport of antimicrobials and antimicrobial resistance genes in soil and runoff following land application of swine manure slurry. Environ Sci Technol 47:12081–12088. https://doi.org/10.1021/es4026358
19. Kay P, Blackwell PA, Boxall AB (2004) Fate of veterinary antibiotics in a macroporous tile drained clay soil. Environ Toxicol Chem. 23:1136–1144. doi: 10.1897/03-374. PMID: 15180364
20. Kay P, Blackwell PA, Boxall ABA (2005) A lysimeter experiment to investigate the leaching of veterinary antibiotics through a clay soil and comparison with field data. Environ Pollut 134:333–341. https://doi.org/10.1016/J.ENVPOL.2004.07.021
21. Krishnasamy V, Otte J, Silbergeld E (2015) Antimicrobial use in Chinese swine and broiler poultry production. Antimicrob Resist Infect Control 4:1–9. https://doi.org/10.1186/s13756-015-0050-y
22. Lei K, Han X, Fu G, Zhao J, Yang L (2014) Mechanism of ofloxacin fluorescence quenching and its interaction with sequentially extracted dissolved organic matter from lake sediment of Dianchi, China. Environ Monit Assess 186:8857–8864. https://doi.org/10.1007/s10661-014-4049-2

23. Li C, Chen J, Wang J, Ma Z, Han P, Luan Y, Lu A (2015) Occurrence of antibiotics in soils and manures from greenhouse vegetable production bases of Beijing, China and an associated risk assessment. Sci Total Environ 521–522:101–107. https://doi.org/10.1016/j.scitotenv.2015.03.070
24. Liu C, Li Z, Berhe AA et al (2019) Characterizing dissolved organic matter in eroded sediments from a loess hilly catchment using fluorescence EEM-PARAFAC and UV–Visible absorption: Insights from source identification and carbon cycling. Geoderma 334:37–48. https://doi.org/10.1016/j.geoderma.2018.07.029
25. Lou Y, Ye ZL, Chen S, Wei Q, Zhang J, Ye X (2018) Influences of dissolved organic matters on tetracyclines transport in the process of struvite recovery from swine wastewater. Water Res 134:311–326. https://doi.org/10.1016/j.watres.2018.02.010
26. Mu G, Ji M, Li S (2018) Evaluation of CDOM sources and their links with antibiotics in the rivers dividing China and North Korea using fluorescence spectroscopy. Environ Sci Pollut Res 25:27545–27560. https://doi.org/10.1007/s11356-018-2773-9
27. Ohno T (2002) Fluorescence inner-filtering correction for determining the humification index of dissolved organic matter. Environ Sci Technol 36:742–746
28. Pan M, Chu LM (2016) Adsorption and degradation of five selected antibiotics in agricultural soil. Sci Total Environ 545–546:48–56. https://doi.org/10.1016/j.scitotenv.2015.12.040
29. Pan M, Chu LM (2017) Leaching behavior of veterinary antibiotics in animal manure-applied soils. Sci Total Environ 579:466–473. https://doi.org/10.1016/j.scitotenv.2016.11.072
30. Qiao M, Chen W, Su J, Zhang B, Zhang C (2012) Fate of tetracyclines in swine manure of three selected swine farms in China. J Environ Sci (China) 24:1047–1052. https://doi.org/10.1016/S1001-0742(11)60890-5
31. Sarmah AK, Meyer MT, Boxall ABA (2006) A global perspective on the use, sales, exposure pathways, occurrence, fate and effects of veterinary antibiotics (VAs) in the environment. Chemosphere 65:725–759. https://doi.org/10.1016/j.chemosphere.2006.03.026
32. Selim HM, Davidson JM, Mansell RS (1976) Evaluation of a two-site adsorption–desorption model for describing solute transport in soil. p. 444–448. In Proc. Summer Computer Simulation Conf., Washington, DC. 12–14 July 1976. Simulation Councils, La Jolla, CA.
33. Šimůnek J, Jacques D, Langergraber G, Bradford SA, Šejna M, Van Genuchten MT (2013) Numerical modeling of contaminant transport using HYDRUS and its specialized modules. J Indian Inst Sci 93:265–284
34. Šimůnek J, van Genuchten M, Šejna M (2008) Development and application of the HYDRUS and STANMOD software packages and related codes. Vadose Zone J 7:587–600. doi:10.2136/vzj2007.0077
35. Song W, Guo M (2014) Residual veterinary pharmaceuticals in animal manures and their environmental behaviors in Soils. In: HE Z and Zhang H (eds.) Applied manure and nutrient chemistry for sustainable agriculture and environment, Springer Netherlands, pp 23–55. DOI 10.1007/978-94-017-8807-6_2

36. Stedmon CA, Bro R (2008) Characterizing dissolved organic matter fluorescence with parallel factor analysis: A tutorial. Limnol Oceanogr Methods 6:572–579. https://doi.org/10.4319/lom.2008.6.572
37. Sukul P, Lamshöft M, Zühlke S, Spiteller M (2008) Sorption and desorption of sulfadiazine in soil and soil-manure systems. Chemosphere 73:1344–1350. https://doi.org/10.1016/j.chemosphere.2008.06.066
38. Sun J, Zeng Q, Tsang DCW, Zhu LZ, Li XD (2017) Antibiotics in the agricultural soils from the Yangtze River Delta, China. Chemosphere 189:301–308. https://doi.org/10.1016/j.chemosphere.2017.09.040
39. Tang X, Liu C, Luo F, Li S, Yang H (2021) Effects of colloidal manure DOM on the transport of antibiotics in calcareous soils. EGU Gen Assem 2021, online, 19–30 Apr 2021, EGU21-9781. https://doi.org/https://doi.org/10.5194/egusphere-egu21-9781, 2021
40. Thiele-Bruhn S (2003) Pharmaceutical antibiotic compounds in soils - A review. J Plant Nutr Soil Sci 166:145–167. https://doi.org/10.1002/jpln.200390023
41. Tong L, Qin L, Xie C, Liu H, Wang Y, Guan C (2017) Distribution of antibiotics in alluvial sediment near animal breeding areas at the Jianghan Plain, Central China. Chemosphere 186:100–107. https://doi.org/10.1016/j.chemosphere.2017.07.141
42. Unold M, Šimůnek J, Kasteel R, Groeneweg J, Vereecken H (2009) Transport of manure-based applied sulfadiazine and its main transformation products in soil columns. Vadose Zo J 8:677–689. https://doi.org/10.2136/vzj2008.0122
43. van Genuchten MT, Wagenet RJ (1989) Two-site/two-region models for pesticide transport and degradation: Th eoretical development and ana lytical solutions. Soil Sci Soc Am J 53:1303–1310
44. Wang HL (2013) Study on soil hydraulic parameters of forest land and sloping farmland in the hilly area of central Sichuan Basin. Northwest A & F University, Yangling, China
45. Wang N, Guo X, Xu J, Hao L, Kong D, Gao S (2015) Sorption and transport of five sulfonamide antibiotics in agricultural soil and soil–manure systems. J Environ Sci Heal - Part B Pestic Food Contam Agric Wastes 50:23–33. https://doi.org/10.1080/03601234.2015.965612
46. Wehrhan A, Kasteel R, Simunek J, Groeneweg J, Vereecken H (2007) Transport of sulfadiazine in soil columns - Experiments and modelling approaches. J Contam Hydrol 89:107–135. https://doi.org/10.1016/j.jconhyd.2006.08.002
47. Wu Z (2019) “Antibiotic use and antibiotic resistance in food-producing animals in China” OECD Food, Agriculture and Fisheries Working Papers. OECD Publ Paris 26 pp
48. Xian Q, Li P, Liu C, Cui J, Guan Z, Tang X (2018) Concentration and spectroscopic characteristics of DOM in surface runoff and fracture flow in a cropland plot of a loamy soil. Sci Total Environ 622–623:385–393. https://doi.org/10.1016/j.scitotenv.2017.12.010
49. Xiao YH, Huang QH, Vähätalo AV, Li FP, Chen L (2014) Effects of dissolved organic matter from a eutrophic lake on the freely dissolved concentrations of emerging organic contaminants. Environ Toxicol Chem 33:1739–1746. https://doi.org/10.1002/etc.2625
50. Xu J, Yu HQ, Sheng GP (2016) Kinetics and thermodynamics of interaction between sulfonamide antibiotics and humic acids: Surface plasmon resonance and isothermal titration microcalorimetry

analysis. J Hazard Mater 302:262–266. https://doi.org/10.1016/j.jhazmat.2015.09.058

51. Yang F, Zhang Q, Jian H et al (2020) Effect of biochar-derived dissolved organic matter on adsorption of sulfamethoxazole and chloramphenicol. J Hazard Mater 396:122598. https://doi.org/10.1016/J.JHAZMAT.2020.122598
52. Yi X, Lin C, Ong EJL, Wang M, Zhou Z (2019) Occurrence and distribution of trace levels of antibiotics in surface waters and soils driven by non-point source pollution and anthropogenic pressure. Chemosphere 216:213–223. https://doi.org/10.1016/j.chemosphere.2018.10.087
53. Zhang W, Tang XY, Weisbrod N, Zhao P, Reid BJ (2015) A coupled field study of subsurface fracture flow and colloid transport. J Hydrol 524:476–488. https://doi.org/10.1016/j.jhydrol.2015.03.001
54. Zhang W, Tang XY, Xian QS, Weisbrod N, Yang JE, Wang HL (2016) A field study of colloid transport in surface and subsurface flows. J Hydrol 542:101–114
55. Zhang Y, Zhang B, He Y et al (2019) DOM as an indicator of occurrence and risks of antibiotics in a city-river-reservoir system with multiple pollution sources. Sci Total Environ 686:276–289. https://doi.org/10.1016/j.scitotenv.2019.05.439
56. Zhao L, Dong YH, Wang H (2010) Residues of veterinary antibiotics in manures from feedlot livestock in eight provinces of China. Sci Total Environ 408:1069–1075. https://doi.org/10.1016/j.scitotenv.2009.11.014
57. Zhao P, Tang X, Zhao P, Wang C, Tang J (2013) Identifying the water source for subsurface flow with deuterium and oxygen-18 isotopes of soil water collected from tension lysimeters and cores. J Hydrol 503:1–10. https://doi.org/10.1016/j.jhydrol.2013.08.033
58. Zhou D, Thiele-Bruhn S, Arenz-Leufen MG, Jacques D, Lichtner P, Engelhardt I (2016) Impact of manure-related DOM on sulfonamide transport in arable soils. J Contam Hydrol 192:118–128. https://doi.org/10.1016/j.jconhyd.2016.07.005
59. Zou Y, Zheng W (2013) Modeling manure colloid-facilitated transport of the weakly hydrophobic antibiotic florfenicol in saturated soil columns. Environ Sci Technol 47:5185–5192. https://doi.org/10.1021/es400624w

Figures

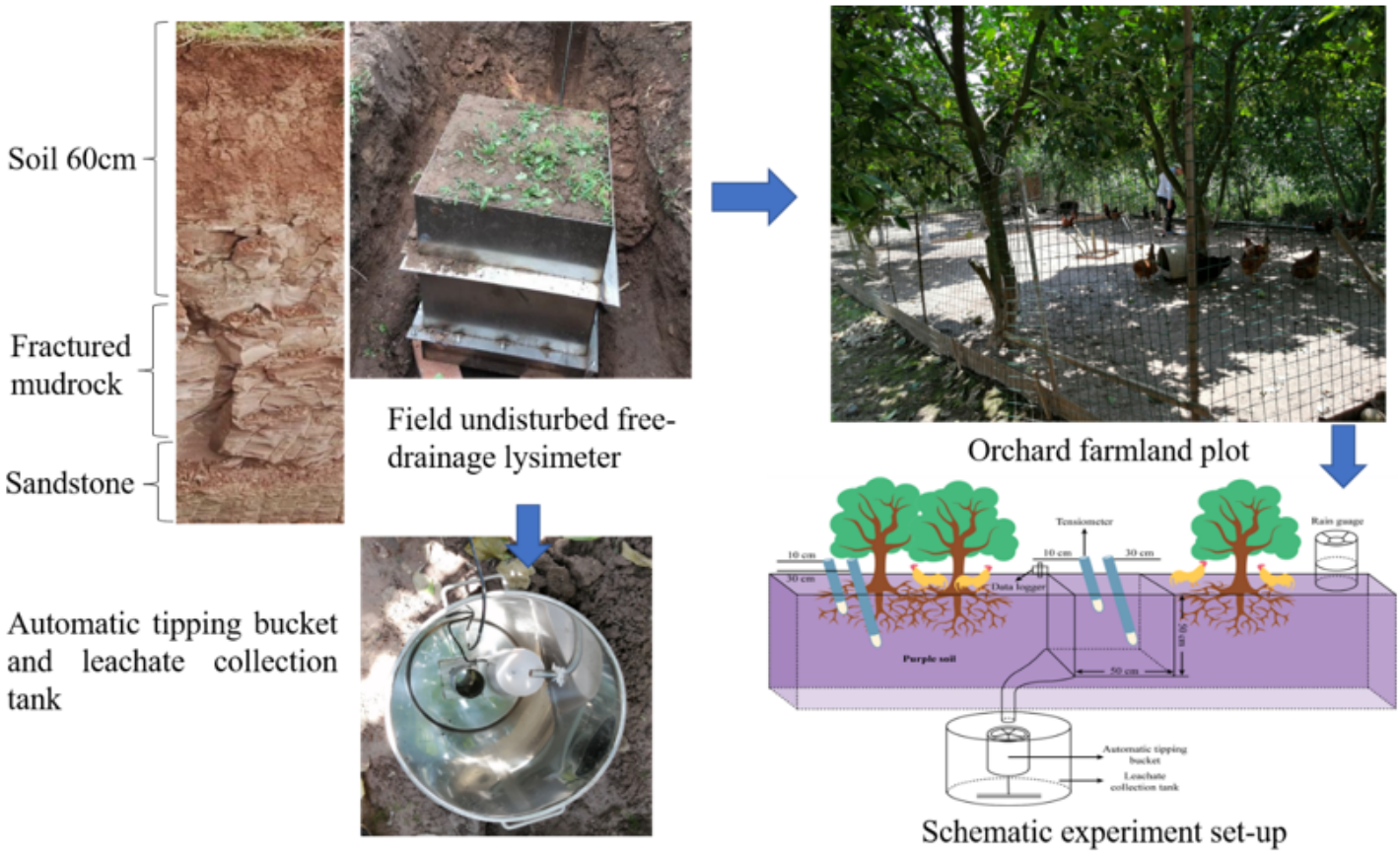

Figure 1

An overview of the chicken-raising orchard plots and the experimental set-up. (Pictures in the upper left are a typical Entisol profile in the studied area and one undisturbed field lysimeter during installation, respectively)

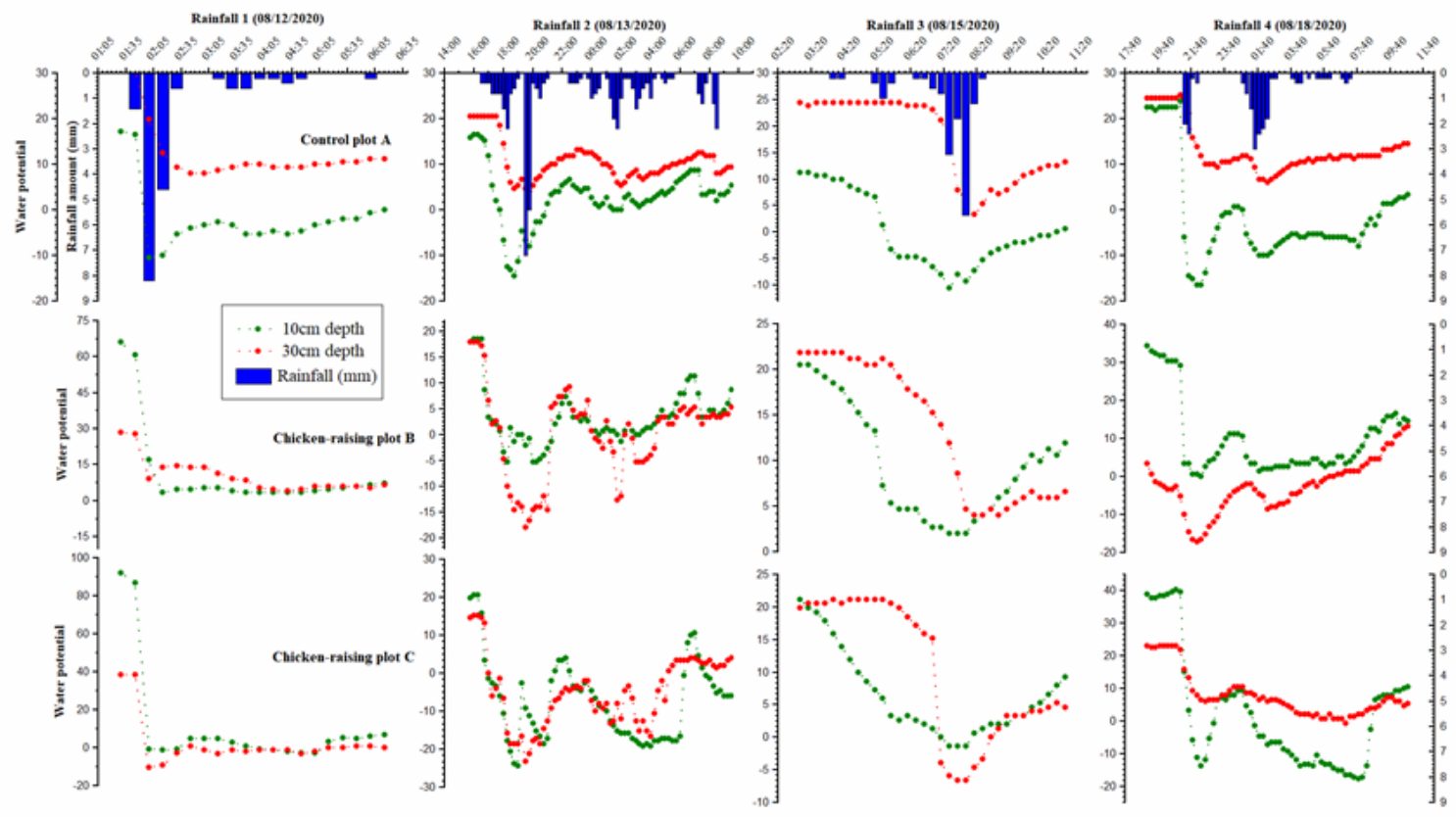

Figure 2

Temporal and spatial variability of water potential dynamics at 10 cm (red line) and 30 cm (green line) depth continuously measured inside the field lysimeter during the observed four rainfall events (I-IV). Control plot A is the plot with no chickens, plots B and C are manured plots (with free-ranging chickens).

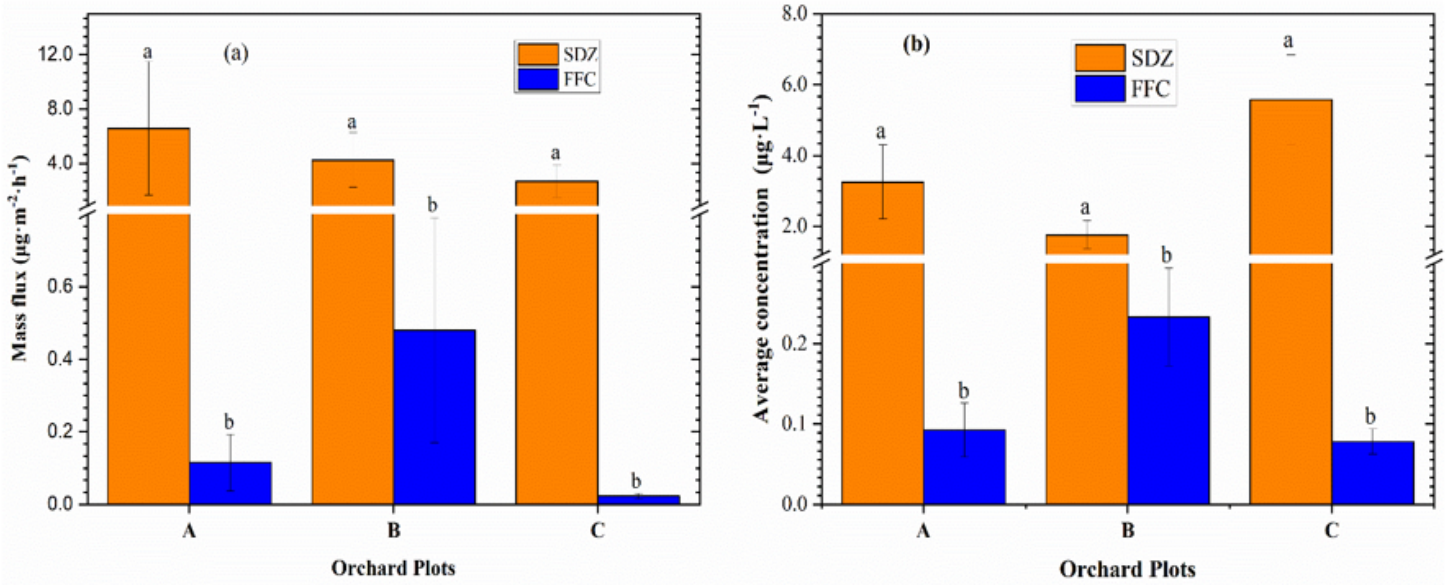

Figure 3

Mean values of (a) mass flux and (b) concentration of sulfadiazine (SDZ) and florfenicol (FFC) in lysimeter leachate from orchard plots during the observed rainfall events. Lowercase letters indicate statistical differences between the antibiotics mass flux (ANOVA $p < 0.05$). A represent control plot (without chickens), B and C are manured plots.

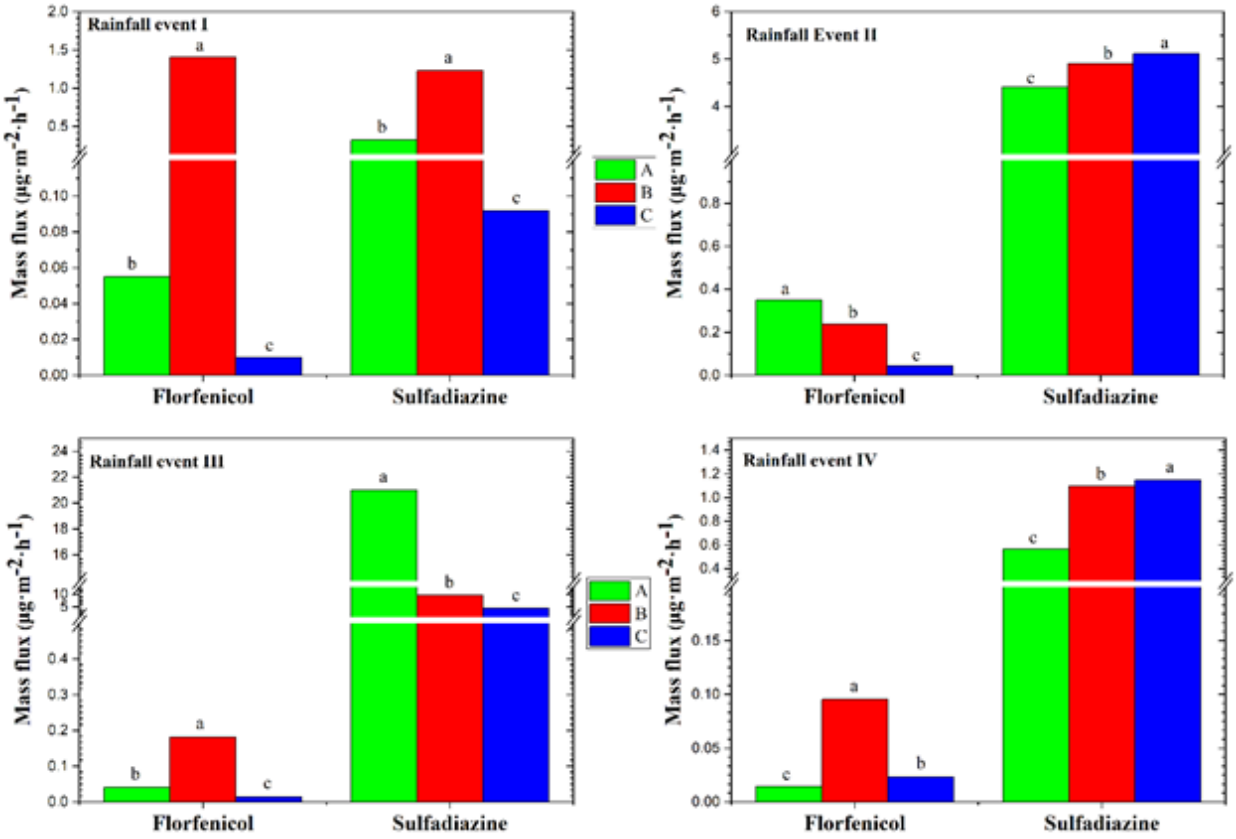

Figure 4

Mass flux of florfenicol (FFC) and sulfadiazine (SDZ) in orchard plots under each rainfall event (I-IV). Lowercase letters indicate statistical differences between the antibiotics mass flux (ANOVA $p < 0.05$). A represent control plot, B and C are manured plots, respectively.

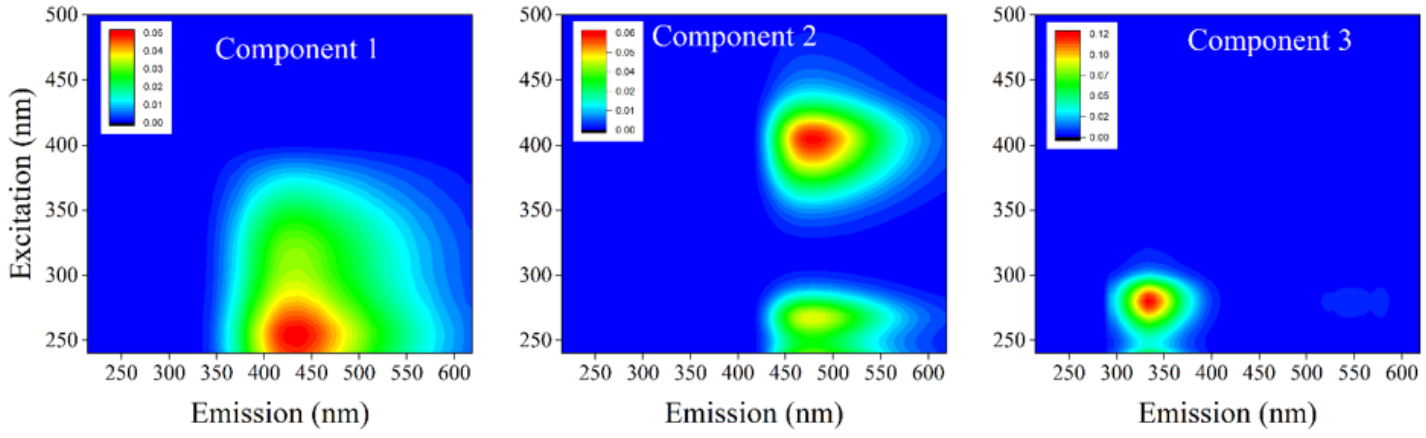

Figure 5

Excitation-emission matrix spectra of three DOM PARAFAC components found in orchard plot leachate. Component 1 (C1) is a short wave humus; Component 2 (C2) is long-wave humus consisting of a humic-like component; and Component 3 (C3) is a tryptophan-like component, respectively.

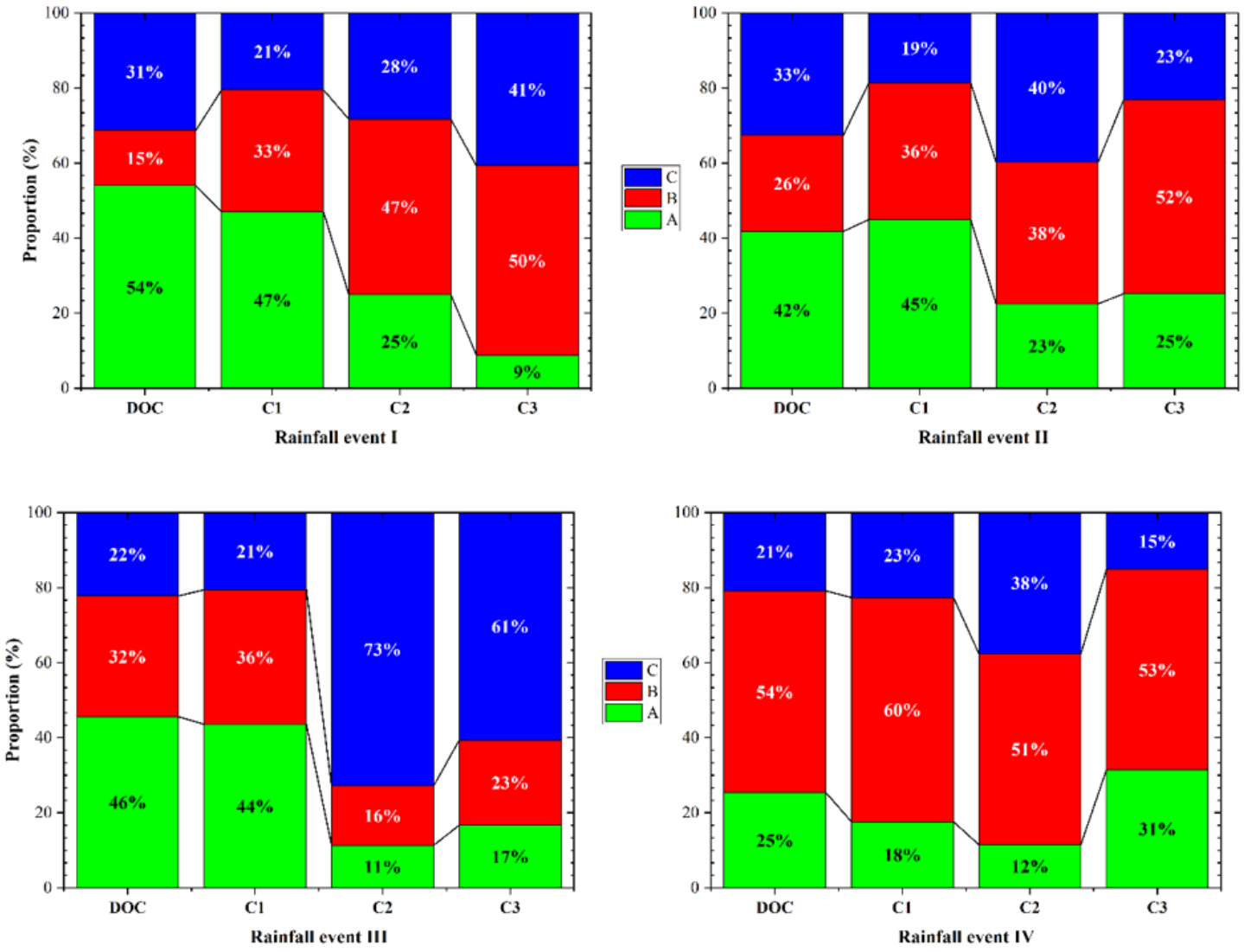

Figure 6

Distribution of DOC values and concentrations of EEM PARAFAC components under natural rainfall events (I-IV). A represent control plot, B and C are manured plots (with free-ranging chickens).

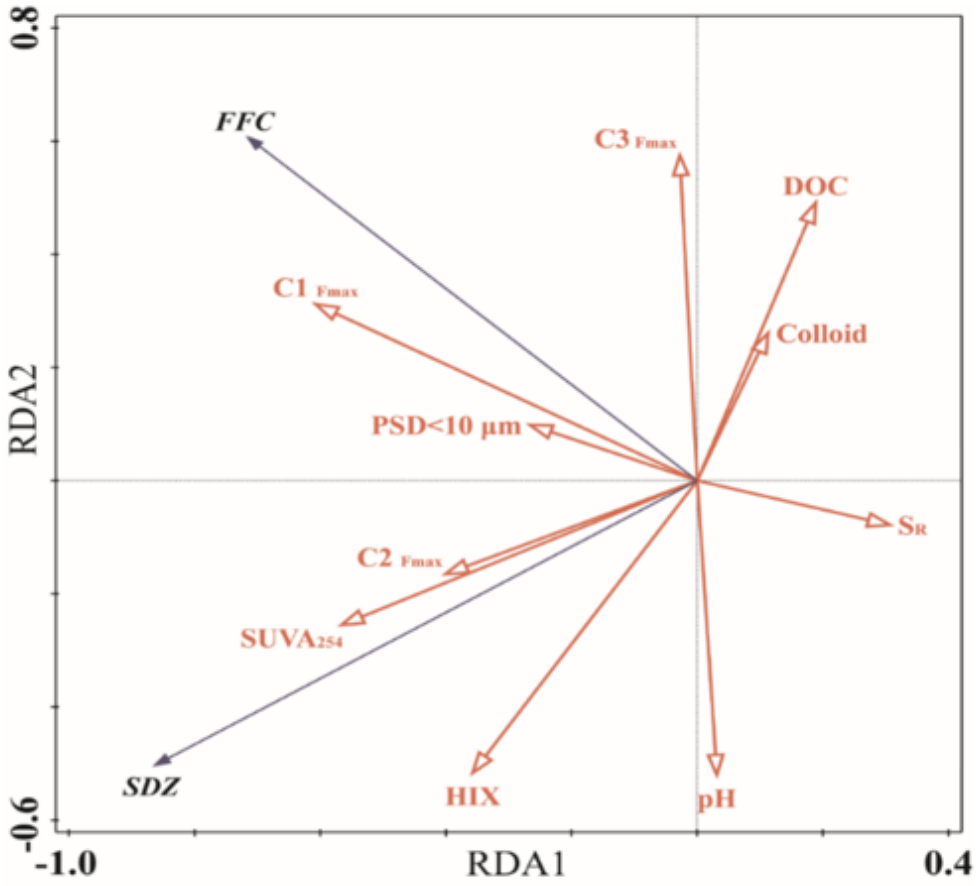

Figure 7

Redundancy analysis (RDA) results showing the relationships between the target antibiotics (black arrows) and soil released colloids and DOM optical indices (red arrows). FFC and SDZ represent florfenicol and sulfadiazine; respectively, C1, C2, and C3 are PARAFAC components, BIX: Biological index, HIX: Humification index, Slope R: slope ratio, SUVA254: specific UV-visible absorbance, $PSD_{<10\ \mu m}$: Sum of particle size distribution <10 μm.

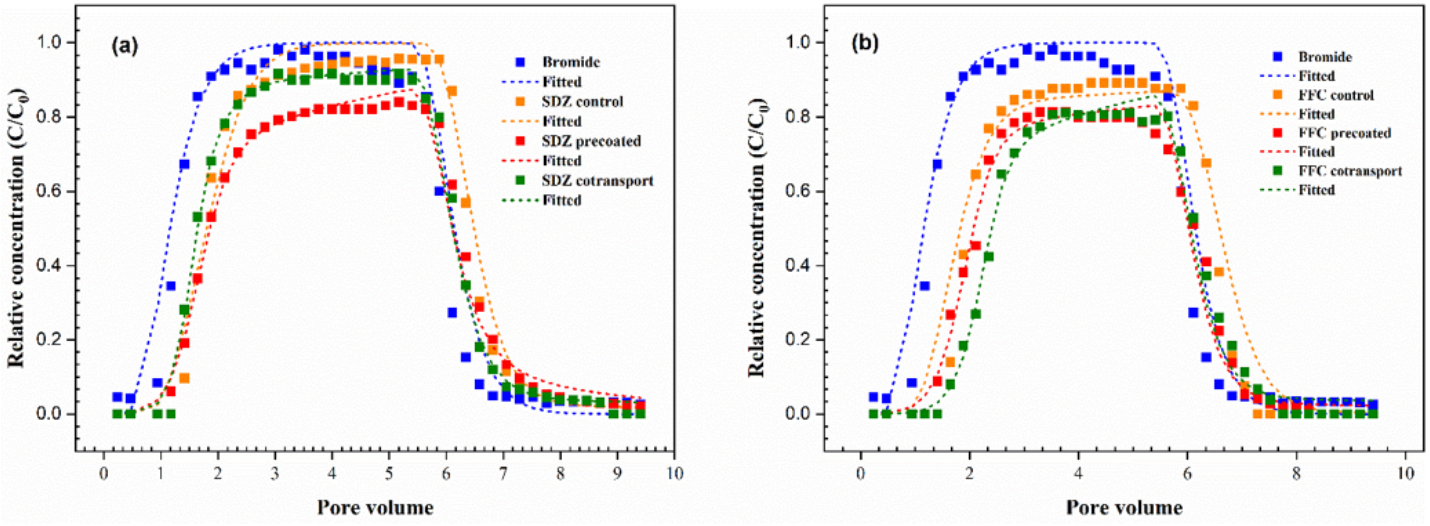

Figure 8

Breakthrough curves of (a) sulfadiazine (SDZ) and (b) florfenicol (FFC) from saturated repacked soil columns with varying manure-DOM treatments fitted to *two kinetics sorption sites model*. Measured (symbols) versus simulated (lines). Bromide was injected as water tracer.

Supplementary Files

This is a list of supplementary files associated with this preprint. Click to download.

- GraphicalAbstract.png
- SupplementaryInformation.docx